

Two-Photon Absorption Properties of Azulenyl Compounds Having a Conjugated Ketone Backbone

Shoichiro Hirakawa,[†] Jun Kawamata,^{*,†} Yasutaka Suzuki,[†] Seiji Tani,[†] Toshihiro Murafuji,[†] Kazuo Kasatani,[‡] Liudmil Antonov,^{§,#} Kenji Kamada,[§] and Koji Ohta[§]

Department of Chemistry, Faculty of Science, Yamaguchi University, Yoshida, Yamaguchi 753-8512, Japan, Department of Advanced Materials Science and Engineering, Faculty of Engineering, Yamaguchi University, Tokiwadai, Ube 755-8611, Japan, and Photonics Research Institute, National Institute of Advanced Industrial Science and Technology (AIST), Midorigaoka, Ikeda, Osaka 563-8577, Japan

Received: January 16, 2008; Revised Manuscript Received: March 7, 2008

Two-photon absorption (TPA) properties of newly synthesized conjugated ketone derivatives that include nonalternant azulenyl moieties in the π -conjugation system, α,α' -bis(1-azulenylidene)cyclopentanone (**1Az**), α,α' -bis(2-azulenylidene)cyclopentanone (**2Az**), and α,α' -bis(6-azulenylidene)cyclopentanone (**6Az**) are reported. TPA spectra of these azulenyl compounds were measured using the open-aperture Z-scan method with a femtosecond laser. The TPA cross section at the peak position ($\sigma^{(2)}_{\text{peak}}$) of **1Az** was found to be the largest among the three azulenyl compounds, which is almost 7 times larger than that of the α,α' -bis(1-naphthylidene)cyclopentanone (**1Nph**), an alternant isomer of **1Az** with the same number of π -electrons. The small detuning energies of the azulenyl compounds compared to those of **1Nph** were responsible for the large TPA cross sections. We report that a compound having an azulenyl moiety can be a promising TPA material.

1. Introduction

In recent years, two-photon absorption (TPA) in molecular systems has attracted increasing attention in relation to various applications such as 3D-microfabrication,^{1–3} optical power limiting,^{4–8} optical data storage,^{2,9–14} two-photon-excited fluorescence imaging,^{15,16} and two-photon photodynamic therapy.^{17,18} In any of these applications, compounds with large TPA cross sections ($\sigma^{(2)}$) are indispensable. Therefore, much effort has been devoted to the development of novel compounds with large $\sigma^{(2)}$.^{19–47} However, the values of $\sigma^{(2)}$ for compounds developed to date still require improvement to meet the requirements of practical applications.

From the perturbation expansion theory, it is well-known that a large $\sigma^{(2)}$ value is obtained for a molecule with large transition dipole moments and/or small detuning energy (ΔE).^{21,41} Thus, a number of efforts have been devoted to increase the transition dipole moments by extension^{19,25,26,32,34,36,42,43,45,47} and the improvement of planarity of the π -conjugated system.^{22,26,37,44} An effective and widely used strategy to enhance the transition dipole moments is the introduction of electron donor (D) and acceptor (A) groups at the ends of the π -conjugated system with asymmetric (D– π –A^{20,23,27,38}) and symmetric (A– π –D– π –A^{19,28,39} or D– π –A– π –D^{19,23,26,27,29,30,40,44}) arrangements. On the basis of this strategy, various kinds of end and central substituents and bridging π -conjugated systems have been examined so far.^{20,23,24,27–30,38–40}

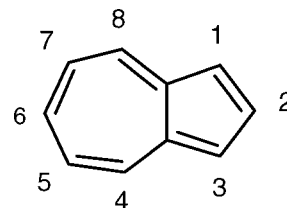


Figure 1. Chemical structure and positional numbering of azulene.

On the one hand, decreasing ΔE is also an effective way to increase $\sigma^{(2)}$. Introduction of D/A groups also leads to a smaller ΔE , due to the lowering of the energy levels of the excited states, resulting in larger $\sigma^{(2)}$.¹⁹ To effectively decrease ΔE , the use of a TPA transition to a higher excited state that is located at almost twice that of the lowest one-photon-absorption (OPA)-allowed excited state has been investigated.^{33,41} This strategy is very effective to decrease ΔE ; however, the high-energy TPA transition often overlaps with an OPA transition band. In such a case, the net absorption is dominated by the contribution from the OPA process, and the advantage of TPA process is diminished in many applications. To overcome this problem and use a small ΔE effectively, a molecular design to control the separation of the excited states is very important.

In this study, we have proposed a strategy for designing a molecule with a small ΔE and large separation in the energy levels of the excited states using the azulenyl moiety. Azulene (Figure 1), a nonalternant and simple hydrocarbon, has unique electronic properties such as high electron affinity, low ionization potential, and low aromatic resonance energy, together with a nonzero dipole moment (0.8 D) whose negative end is toward its five-membered ring.⁴⁸ Furthermore, azulene exhibits an interesting spectroscopic property; the main absorption band of azulene is assigned to the transition from the ground state (S_0) to the second one-photon excited state (S_2), which is well

* Author to whom correspondence should be addressed. Telephone and fax: +81-83-933-5729. E-mail address: j_kawa@yamaguchi-u.ac.jp.

[†] Faculty of Science, Yamaguchi University.

[‡] Faculty of Engineering, Yamaguchi University.

[§] National Institute of Advanced Industrial Science and Technology (AIST).

[#] Present address: Institute of Organic Chemistry, Bulgarian Academy of Sciences, Acad. G. Bonchev str. bl. 9, Sofia 1113, Bulgaria.

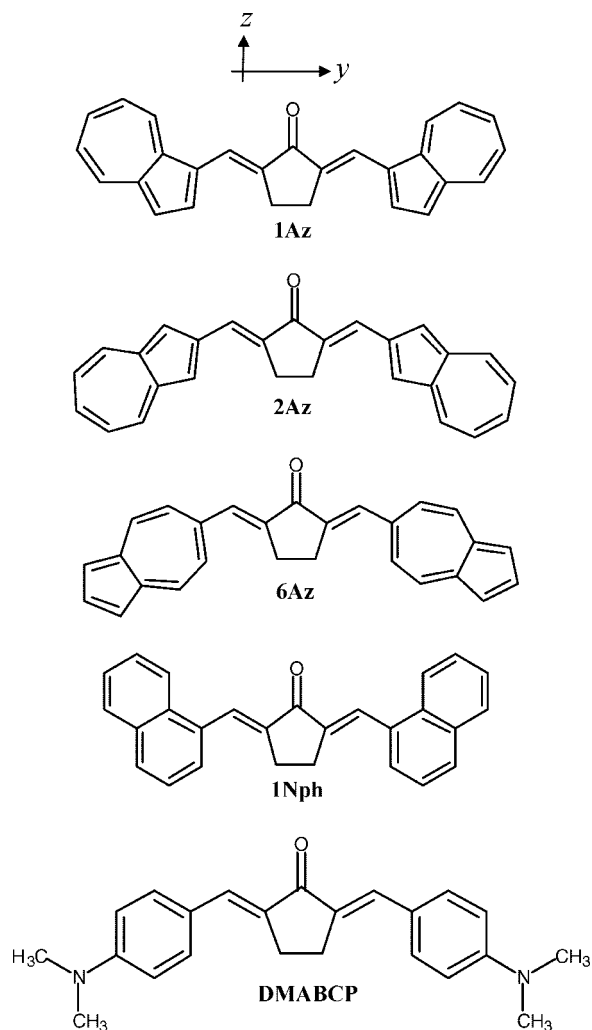


Figure 2. Molecular structures of the conjugated ketone derivatives examined. Molecular axes used for DFT calculations are also shown.

separated from the very weak transition from S_0 to the first one-photon excited state (S_1).⁴⁹ Because S_1 is located almost halfway between S_2 and S_0 , the electronic features specific to azulene are suitable for obtaining small ΔE with regard to the S_2 related TPA transition.

Unsubstituted azulene must have a small $\sigma^{(2)}$ value because of the shorter length of its π -electron system, compared with those of efficient TPA chromophores. However, this drawback can be overcome by incorporating an azulenyl moiety in a large and planar π -electron system. This incorporation provides a large transition moment, in addition to the small ΔE of the azulenyl groups, so that an excellent TPA property is expected. Of note is a large value of $\sigma^{(2)}$ that was very recently reported for a compound having azulene rings fused to a porphyrin ring.⁵⁰

From this investigation, we report OPA and TPA characteristics of azulenyl derivatives incorporated with a conjugated ketone, bis(ethylidene)cyclopentanone. The derivatives have two azulenyl groups in symmetric fashion, at both ends of the conjugated ketone (Figure 2). The conjugated ketone backbone bears the five-membered ring at its center, which provides excellent planarity⁵¹ throughout the conjugated chain. Compounds with this backbone are known to exhibit large TPA cross sections.^{26,40}

Derivatives with different substitution positions of the azulenyl groups, α,α' -bis(n -azulenylidene)cyclopentanone ($n\text{Az}$)

where $n = 1, 2,$ and 6 positions (see Figure 1), were systematically investigated. It was reported that an azulenyl group acts as a donor when the position at the electron-rich five-membered ring is introduced into a π -electron system.⁵² For example, the azulen-1-yl moiety is known to have an efficient electron donating ability, which promotes intramolecular charge transfer from the azulen-1-yl moiety.^{52,53} Some compounds bearing the azulen-1-yl moiety have been reported to exhibit salient second-order optical nonlinearities,^{52–54} because of the intermolecular charge transfer. At the same time, the keto group of the backbone acts as an electron acceptor (A). Thus, symmetric charge transfer from the donor groups at both terminals to the $-\pi-A-\pi-$ backbone can be expected for **1Az**. The same behavior is also expected for **2Az**, but in a different magnitude, because of the difference in the electron donating ability. On the other hand, when a position at the seven-membered ring of azulenyl group is introduced into a π -conjugated system, the azulenyl group would act as an electron acceptor.⁵² Therefore, **6Az** was investigated for comparison.

In addition to the azulenyl compounds, compounds having similar structures, but without the azulenyl moiety as a reference, such as α,α' -bis(1-naphthylidene)cyclopentanone (**1Nph**) and α,α' -bis(p -(dimethylamino)benzylidene)cyclopentanone (**DMABCP**), were also investigated. The former, which has naphthyl groups instead of azulenyl groups, is an alternant structural isomer with the same number of π -electrons. The latter has (dimethylamino)phenyl groups, which have a Hammett's constant similar to that of the azulen-1-yl group,⁵² and thus, these groups are expected to have a similar electron donating ability.

The TPA spectra of these compounds were measured by the femtosecond open-aperture Z-scan method⁵⁵ for a wide range of wavelength (600–1100 nm). The magnitudes of $\sigma^{(2)}_{\text{peak}}$ for three azulene derivatives were found to be considerably different from each other, depending on the substitution position of the azulenyl group; **1Az** exhibited the largest $\sigma^{(2)}_{\text{peak}}$ followed by **2Az** and then **6Az**. The value of $\sigma^{(2)}_{\text{peak}}$ for **1Nph** was smaller than that for the azulenyl compounds; however, **DMABCP** exhibited the largest $\sigma^{(2)}_{\text{peak}}$ among all the compounds measured in this study. The electronic states of these azulenyl compounds were assigned using the results of time-dependent density functional theory (TDDFT) calculations. The ΔE 's of the compounds examined in this study were estimated from the energies of the electronic states between the first OPA-allowed and the first TPA-allowed states.

2. Experiments

Materials. The conjugated ketone derivatives were synthesized by the base-catalyzed cross-aldol condensation reaction of cyclopentanone (1 mmol) with the corresponding aldehydes (2 mmol) in 100 mL of ethanol and in the presence of a catalytic amount of NaOH. All syntheses were performed at room temperature. The crude products were purified several times by recrystallization from chloroform. The purity was determined using thin layer chromatography (TLC) on silica gel. The chemical structures of the products were confirmed by ¹H NMR spectra recorded on a Bruker Avance 400 spectrometer in CDCl₃ with tetramethylsilane (TMS) as an internal standard.

α,α' -Bis(1-azulenylidene)cyclopentanone (1Az). Purple solid, yield 28%, ¹H NMR (CDCl₃): $\delta = 3.28$ (4H, s), 7.30 (2H, t, $J = 9.7$ Hz), 7.39 (2H, t, $J = 9.9$ Hz), 7.52 (2H, d, $J = 4.2$ Hz), 7.72 (2H, t, $J = 9.8$ Hz), 8.28 (2H, d, $J = 4.2$ Hz), 8.35 (2H, s), 8.36 (2H, d, $J = 8.8$ Hz), 8.87 (2H, d, $J = 9.8$ Hz). Anal. Calcd for C₂₇H₂₀O (360.45): C, 89.97; H, 5.59; O, 4.44. Found: C, 89.72; H, 5.69.

α,α' -Bis(2-azulenylidene)cyclopentanone (2Az). Green solid, yield 14%, $^1\text{H NMR}$ (CDCl_3): $\delta = 3.34$ (4H, s), 7.20 (4H, t, $J = 9.8$ Hz), 7.58 (2H, t, $J = 10.0$ Hz), 7.59 (4H, s), 7.98 (2H, s), 8.33 (4H, d, $J = 9.6$ Hz). Anal. Calcd for $\text{C}_{27}\text{H}_{20}\text{O}$ (360.45): C, 89.97; H, 5.59; O, 4.44. Found: C, 89.87; H, 5.71.

α,α' -Bis(6-azulenylidene)cyclopentanone (6Az). Green solid, yield 12%, $^1\text{H NMR}$ (CDCl_3): $\delta = 3.23$ (4H, s), 7.42 (4H, d, $J = 10.6$ Hz), 7.43 (4H, d, $J = 3.7$), 7.81 (2H, s), 7.97 (2H, t, $J = 3.7$), 8.36 (4H, d, $J = 10.6$ Hz). Anal. Calcd for $\text{C}_{27}\text{H}_{20}\text{O}$ (360.45): C, 89.97; H, 5.59; O, 4.44. Found: C, 89.87; H, 5.76.

Optical Measurements. OPA spectra of the compounds were measured for solutions in chloroform using a Hitachi U-3300 spectrophotometer with a 1 cm quartz cuvette. The oscillator strengths were calculated assuming a Gaussian band shape from the OPA spectra. The solvent effects of the OPA spectra for azulene derivatives were investigated by comparison of the OPA spectra taken in chloroform, dimethyl sulfoxide (DMSO), and 1-methylnaphthalene.

TPA spectra were measured by the open-aperture Z-scan method.⁵⁵ Details of the setup for the Z-scan measurements and the analysis procedures have been described previously,⁵⁶ and thus are only briefly mentioned. A parametric amplifier (Spectra-Physics, OPA-800) pumped by a femtosecond regenerative amplifier (Spectra-Physics, Spitfire) was used as a wavelength-tunable light source. The typical pulse duration was 120–140 fs with a repetition rate of 1 kHz. The incident beam was focused by a plano-convex lens ($f = 150$ mm) and the sample solutions held in a quartz cuvette were scanned along the propagation axis of the incident beam. The path length of the cuvette was selected as 1 or 2 mm, depending on the sample concentration and the magnitude of the cross section. This is shorter than the Rayleigh range of the setup ($z_R = 4$ –9 mm, depending on the wavelength), which fulfills the optically thin condition. The average incident power was varied from 0.05 to 0.7 mW, which corresponds to the on-axis peak powers of 25–347 GW/cm^2 . Proportionality relations between the TPA absorbance q_0 and the incident power, that is, the on-axis peak power, were confirmed at each measurement. The sample concentrations were made to be as high as possible to improve the signal-to-noise ratio in the Z-scan measurements, and thus the solvents were chosen depending on the compounds. The concentrations used were 3.6×10^{-4} mol/L in DMSO for **1Az**, 1.2×10^{-3} mol/L in chloroform for **2Az**, 1.1×10^{-3} mol/L in 1-methylnaphthalene for **6Az**, 1.7×10^{-2} mol/L in chloroform for **1Nph**, and 1.7×10^{-3} mol/L in chloroform for **DMABCP**. The TPA spectra were measured in the wavelength range from 600 to 1100 nm of the incident light.

Theoretical Calculations. The density functional theory (DFT) calculations were performed using the Gaussian 03 program package.⁵⁷ The molecular structures of the three azulenyl compounds belonging to the C_2 and C_{2v} point groups were optimized at the B3LYP level of theory using the 6-31G(d) basis set. The molecular axes used for the calculations are shown in Figure 2. The point groups of the more stable optimized structures of **1Az** and **2Az** were C_{2v} , and that for **6Az** was C_2 . For the C_2 molecules, the azulenyl moieties were held as planar to facilitate the geometric optimizations. The TDDFT method was used to obtain the OPA properties of the azulenyl compounds at their optimized geometries in the ground state; excitation energies, transition dipole moments and oscillator strengths between the ground and singlet excited states were calculated at the B3LYP level of theory using the 6-31+G(d) basis set.

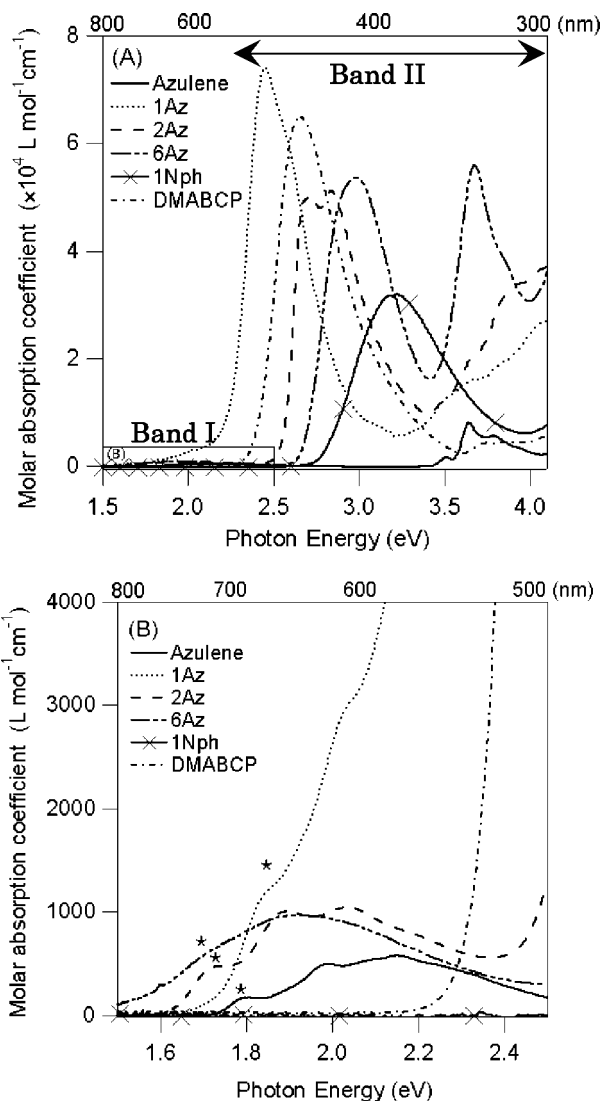


Figure 3. One-photon absorption spectra of unsubstituted azulene, azulenyl compounds, **1Nph**, and **DMABCP** in chloroform at room temperature (A). Detailed band I region of unsubstituted azulene and azulenyl compounds (B). The asterisk indicates positions of the 0–0 band.

3. Results and Discussion

One-Photon Absorption Properties. The OPA spectra of “unsubstituted” azulene and the five conjugated ketene compounds in chloroform solution are shown in Figure 3A, and the expanded wavelength range of 500–800 nm (2.5–1.5 eV) is shown in Figure 3B. The azulenyl compounds were found to have broad and weak absorption bands similar to that of unsubstituted azulene, as shown in Figure 3B, although it was not clear for **1Az** due to the large overlap with a strong absorption band around 500 nm (2.5 eV). The absorption bands observed in the wavelength range of 500–800 nm are referred to as band I. Intense absorption bands found in the wavelength range of 300–520 nm (4.1–2.4 eV) are referred to as band II. The absorption bands of **1Nph** and **DMABCP** were not observed in the wavelength range of band I, but in the wavelength range of band II. The excitation energies (E) and molar absorption coefficients (ϵ) at the absorption peaks, and oscillator strengths (f) of the absorption band are summarized in Table 1.

In the case of unsubstituted azulene, band I has been assigned to the $S_0 \rightarrow S_1$ transition.^{49,58} The fine structure of band I can

TABLE 1: Energies at Peak Positions (E), Molar Absorption Coefficients (ϵ), and Oscillator Strengths (f) of Unsubstituted Azulene and Azulenyl Compounds in Chloroform Solution^a

compound	band I			band II		
	E (eV)	ϵ (L mol ⁻¹ cm ⁻¹)	f	E (eV)	ϵ (L mol ⁻¹ cm ⁻¹)	f
azulene	1.79	170	0.011	3.64	8100	0.088
1Az	1.85	490	0.023	2.44	73600	1.354
2Az	1.72	330	0.019	2.70	49800	1.291
6Az	1.70	280	0.011	2.98	53500	1.078
1Nph				3.22	32000	0.571
DMABCP				2.65	64900	1.114

^a In the case of E and ϵ of band I, the values at the peaks of the 0–0 transitions are shown. The f of band I and band II were estimated from the integrated value of all ϵ corresponding to the respective band region. ϵ and f were calculated assuming a Gaussian band shape.

be interpreted as a vibronic progression. Similar fine structures were also observed for all the azulenyl compounds. The positions of the 0–0 transitions are marked by asterisks in Figure 3B. The differences in the 0–0 transition energies of band I between the azulenyl compounds and unsubstituted azulene were relatively small (<0.1 eV). In addition, the values of the ϵ of the 0–0 transitions and the oscillator strengths for the absorption in band I for unsubstituted azulene and the azulenyl compounds were in the same order of magnitude. Therefore, the characteristic transitions of band I for the azulenyl compounds are considered to be similar to that for unsubstituted azulene. In other words, band I did not show a significant change, even when the π -conjugated system was extended.

On the other hand, band II for the azulenyl compounds was found to show a significant red shift compared to that of unsubstituted azulene (Figure 3A). The nonazulenyl compounds also exhibit strong absorption peaks in the band II region (385 nm (3.22 eV) for **1Nph**, and 467 nm (2.65 eV) for **DMABCP**). It was comprehensively reported that for bis(arylalkylidene)cycloalkanones the peak wavelength of the lowest-energy transition is red-shifted, and the oscillator strengths are increased when the conjugation of the π -electron system is enhanced.^{59,60} The large red shifts found for band II of the azulenyl compounds suggest that the π -electrons in the azulenyl moieties are well conjugated with the central $-\pi-A-\pi-$ system and that the π -conjugation is extended throughout the entire molecule.

It is known that some efficient TPA molecules show significant solvatochromism.⁶¹ Therefore, solvent effects on the absorption spectra of the azulenyl compounds were examined. The peak positions of **1Az**, **2Az**, and **6Az** observed in chloroform, DMSO, and 1-methylnaphthalene were almost the same as each other. Thus, the solvatochromic effect is negligible for these compounds.

Two-Photon Absorption Properties of Azulenyl Compounds. Open-aperture Z-scan measurements were conducted with concentrated solutions of the compounds. The solvent effects on the OPA characteristics of the **1Az**, **2Az**, and **6Az** azulenyl compounds were negligible; therefore, it is reasonable that the TPA properties can be compared with each other even though they are evaluated in different solvents.

The TPA cross section spectra obtained are provided in Figure 4. The azulenyl compounds exhibited strong TPA in the wavelength region employed. A relatively weak TPA peak or shoulder (but still on the order of a few hundred GMs, where 1 GM = 1 \times 10⁻⁵⁰ cm⁴ s molecule⁻¹ photon⁻¹) was observed for **1Az** and **6Az** at around 1.4 eV. In addition, $\sigma^{(2)}$ was found

to increase significantly with increasing photon energy, larger than 1.6 eV, for each azulenyl compound. The maximum values ($\sigma^{(2)}_{\text{max}}$) observed at the highest photon energy employed were close to 1000 GM or more (3280 GM for **1Az**, 920 GM for **2Az**, and 860 GM for **6Az**). The spectral region where significant increases in $\sigma^{(2)}$ are observed overlaps with band I of the OPA and is also close to the intense band II. Therefore, these increases are considered to arise from resonance enhancement, *i.e.*, the increase of TPA transition probability due to the double resonance of the OPA- and TPA-allowed excited states.²⁸ On the other hand, the relatively weak TPA peaks observed at ca. 1.4 eV are considered to be the lowest energy TPA transitions. The peak is not clear for **2Az**, because of the large overlap with the much stronger TPA band at higher energy. However, it is logical to consider that there is a TPA peak at almost the same transition energy, due to the similarity of the electronic structure of **2Az** with the other azulenyl compounds. Contrary to the azulenyl compounds, the nonazulenyl compounds, **1Nph** (Figure 4D) and **DMABCP** (Figure 4E), exhibit quite different TPA spectra. These two compounds show a single distinct TPA peak in the spectral region observed. The peak $\sigma^{(2)}$ value ($\sigma^{(2)}_{\text{peak}}$) for **DMABCP** (ca. 760 GM at 1.54 eV) is much larger than that for **1Nph** (ca. 40 GM at 1.73 eV). The unsubstituted azulene solution was also measured; however, no measurable TPA signals were obtained.

The large $\sigma^{(2)}_{\text{max}}$ values of the azulenyl compounds in the double resonance region are very interesting; nevertheless, hereafter we concentrate on the lowest energy TPA transition, because the main aim of this paper is the comparative study of the structure–property relationship among these compounds, which can be discussed more clearly with the lowest-energy transitions. However, the transitions do not always provide a distinct spectral peak as shown in Figure 4, due to overlap with the strong double resonance bands. Therefore, the contribution of the lowest-energy peak to the total spectral intensity was estimated with the four-state model.²⁸ This model assumes two competitive TPA transitions with different final states (e_1 and e_2), but mediated with the same OPA-allowed state (k), both contributing to the cross section observed at a photon energy of E_p , and is expressed as

$$\sigma^{(2)}(E_p) \propto \frac{E_p^2}{(E_{kg} - E_p)^2 + \Gamma_{kg}^2} \times \left[\frac{A_1}{(E_{e_1g} - 2E_p)^2 + \Gamma_{e_1g}^2} + \frac{A_2}{(E_{e_2g} - 2E_p)^2 + \Gamma_{e_2g}^2} \right] \quad (1)$$

where E_{kg} , E_{e_1g} , and E_{e_2g} are transition energies from the ground state (g) to k , e_1 , and e_2 , respectively. $A_1 = |\mu_{e_1k}|^2 |\mu_{kg}|^2 \Gamma_{e_1g}$, $A_2 = |\mu_{e_2k}|^2 |\mu_{kg}|^2 \Gamma_{e_2g}$, where μ_{kg} and μ_{e_1k} are the transition dipole moments between corresponding states, and Γ is the corresponding damping factor. Here, all parameters were treated as fitting parameters. The contributions of the lowest-energy peak obtained from the best fits are shown with dotted lines in Figure 4, and the best-fit parameters are listed in Table 2. Setting A_2 to zero reduced eq 1 to the simple three-state model, which was applied for **1Nph** and **DMABCP**. The results are shown with solid lines in Figure 4 and listed in Table 2. The values of E_{kg} were found to reasonably close to the transition energies of band I obtained by the OPA measurements. Thus, the OPA-allowed excited state is the major intermediate state of the lowest energy TPA transition.

Molecular Orbital Calculations and Assignment of the Experimentally Observed Excited States. The calculated results of the excitation energies, orbital pictures of the

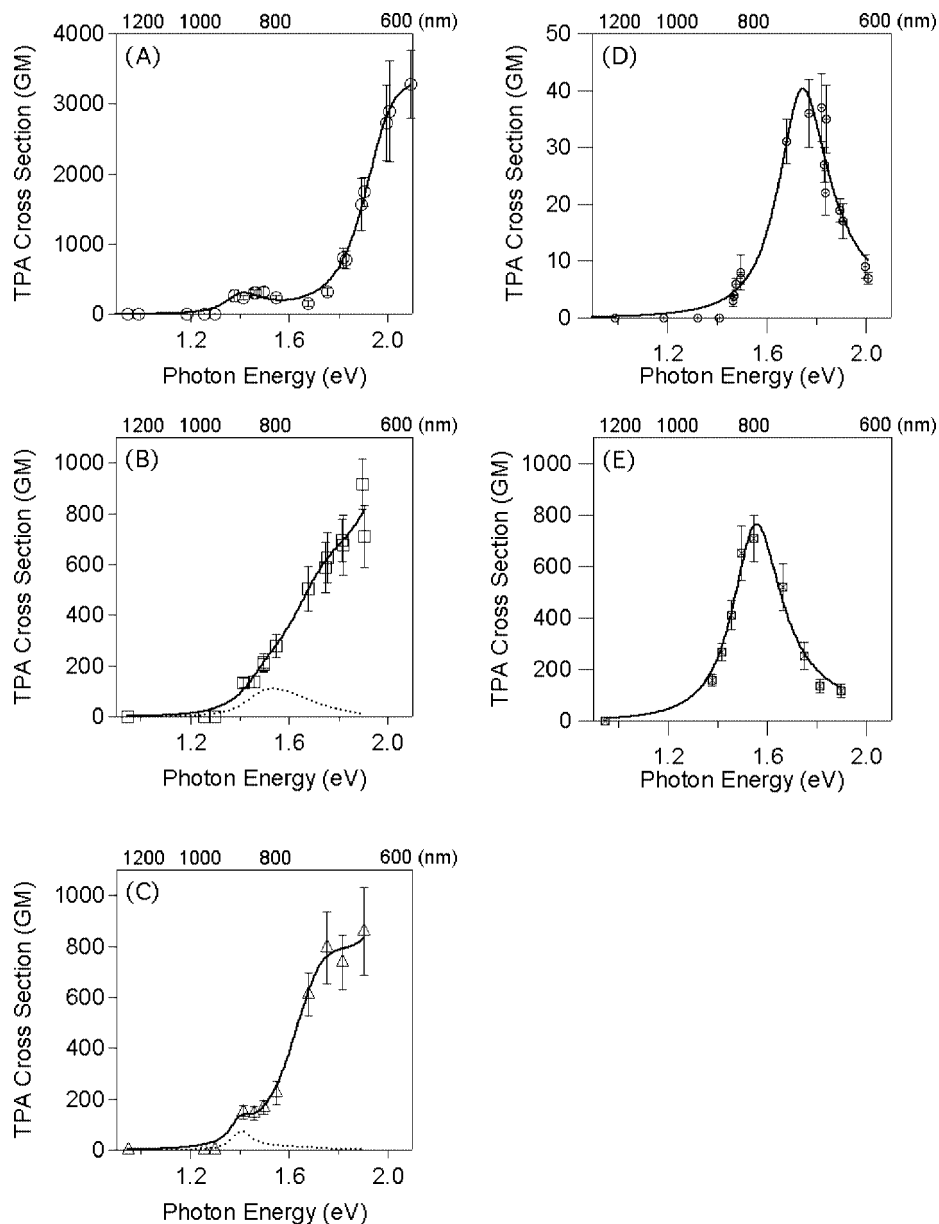


Figure 4. TPA spectra of (A) **1Az** in dimethyl sulfoxide, (B) **2Az** in chloroform, (C) **6Az** in 1-methylnaphthalene, (D) **1Nph** in chloroform, and (E) **DMACCP** in chloroform. Curve fits were performed using the four-state models (solid line). One GM = 1×10^{-50} cm⁴ s molecule⁻¹ photon⁻¹.

TABLE 2: TPA Cross Section Maxima ($\sigma^{(2)}_{\max}$), Photon Energies at the Position of $\sigma^{(2)}_{\max}$ (E_{\max}), and the TPA Cross Section at the Peak Position of the Best Curve Fit Calculated by the Four-State Model with Two Final States ($\sigma^{(2)}_{\text{peak}}$)^a

compound	solvent	$\sigma^{(2)}_{\max}$, GM	E_{\max} , eV	$\sigma^{(2)}_{\text{peak}}$, GM	E_{kg} , eV	E_{e1g} , eV	ΔE , eV
1Az	dimethyl sulfoxide	3280	2.09	270 ± 40	1.97	2.79	0.57
2Az	chloroform	920	1.90	110 ± 30	1.68	2.96	0.20
6Az	1-methylnaphthalene	860	1.90	70 ± 30	1.68	2.80	0.28
1Nph	chloroform			40 ± 6	3.22	3.46	1.49
DMABCP	chloroform			760 ± 90	2.65	3.09	1.12

^a Best fit values of the energies for transition between the ground and first one-photon-allowed excited states (E_{kg}) and the energies for transition between the ground and first TPA states (E_{e1g}) are also listed. The detuning energies (ΔE) shown here were estimated using E_{kg} and E_{e1g} . One MG = 1×10^{-50} cm⁴ s molecule⁻¹ photon⁻¹.

excitation, oscillator strengths, and transition dipole moments for the azulenyl compounds are summarized in Tables 3–5. The calculated excitation energies are summarized in the energy level diagrams (Figure 5) together with the energy levels of the excited states obtained from the OPA and TPA measurements. As shown in Figure 5, there are some near degenerate excited states. This is reasonable, because the azulenyl compounds have

two identical chromophores, *i.e.*, azulenyl moieties at both ends of the π -conjugated system. The lowest excited states (S_1 and S_2) are near degenerate for all azulenyl compounds.

First, we examine transitions from the ground state to the near degenerate lowest excited states. These two near degenerate transitions are considered to correspond to the experimentally observed lowest-energy OPA transition. Considering Tables 3–5,

TABLE 3: One-Photon Absorption Properties of 1Az Calculated Using the TDDFT Method

n	excitation energy $\Delta E[S_n - S_0]$ (eV)	symmetry	orbital picture ^a	transition dipole moment (au)	oscillator strength
1	2.04	B ₂	a ₂ (H) → b ₁ (L) (0.85) b ₁ (H-1) → a ₂ (L+1) (-0.44)	-0.208 (y)	0.0022
2	2.04	A ₁	a ₂ (H) → a ₂ (L+1) (0.85) b ₁ (H-1) → b ₁ (L) (-0.44)	0.3308 (z)	0.0055
3	2.57	B ₂	a ₂ (H) → b ₁ (L+2) (0.91)	-4.6345 (y)	1.3535
4	2.65	A ₁	b ₁ (H-1) → b ₁ (L) (0.88) a ₂ (H) → a ₂ (L+1) (0.47)	-0.0722 (z)	0.0003
5	2.65	B ₂	b ₁ (H-1) → a ₂ (L+1) (0.88) a ₂ (H) → b ₁ (L) (0.47)	0.3357 (y)	0.0073
6	2.92	A ₁	b ₁ (H-1) → b ₁ (L+2) (0.83) a ₂ (H) → a ₂ (L+3) (-0.47)	-0.0416 (z)	0.0010
7	2.92	A ₂	b ₂ (H-2) → b ₁ (L+2) (0.94)		0
8	3.25	A ₁	a ₂ (H) → a ₂ (L+3) (0.72) a ₂ (H-3) → a ₂ (L+1) (0.35) b ₁ (H-4) → b ₁ (L) (0.35) b ₁ (H-1) → b ₁ (L+2) (0.30)	0.4955 (z)	0.0196

^a Values in parentheses are the coefficients of each electronic configuration contributing to the excited state. Configuration coefficients >0.3 are listed. Data for $n = 1, 2, 4, 5,$ and 8 show the transitions corresponding to local excitations.

TABLE 4: One-Photon Absorption Properties of 2Az Calculated Using the TDDFT Method

n	excitation energy $\Delta E[S_n - S_0]$ (eV)	symmetry	orbital picture ^a	transition dipole moment (au)	oscillator strength
1	2.08	B ₂	a ₂ (H) → b ₁ (L) (0.89) b ₁ (H-1) → a ₂ (L+1) (-0.35)	0.4205 (y)	0.0090
2	2.08	A ₁	b ₁ (H-1) → b ₁ (L) (0.89) a ₂ (H) → a ₂ (L+1) (-0.35)	0.4459 (z)	0.0101
3	2.65	B ₂	a ₂ (H-2) → b ₁ (L) (0.91)	-4.4591 (y)	1.2906
4	2.69	A ₂	b ₂ (H-4) → b ₁ (L) (0.95)		0
5	2.74	A ₁	a ₂ (H) → a ₂ (L+1) (0.89) b ₁ (H-1) → b ₁ (L) (0.40)	-0.1582 (z)	0.0017
6	2.75	B ₂	b ₁ (H-1) → a ₂ (L+1) (0.89) a ₂ (H) → b ₁ (L) (0.40)	-0.2785 (y)	0.0052
7	2.97	A ₁	b ₁ (H-3) → b ₁ (L) (0.81) a ₂ (H-2) → a ₂ (L+1) (-0.55)	-0.4106 (z)	0.0123
8	3.25	A ₁	a ₂ (H-2) → a ₂ (L+1) (0.69) b ₁ (H-3) → b ₁ (L) (0.37) a ₂ (H) → a ₂ (L+3) (0.34) b ₁ (H-1) → b ₁ (L+2) (0.34)	-0.500 (z)	0.0199

^a Values in parentheses are the coefficients of each electronic configuration contributing to the excited state. Configuration coefficients >0.3 are listed. Data for $n = 1, 2, 5, 6,$ and 8 show the transitions corresponding to local excitations.

the $S_0 \rightarrow S_1$ transitions are governed by the one-electron excitation from the highest occupied molecular orbital (HOMO) to the lowest unoccupied molecular orbital (LUMO) for all the azulenyl compounds. Contrary to this, the MO's involved in the $S_0 \rightarrow S_2$ transition for **1Az** are different from that for **2Az** and **6Az**, but with some regularity. The main contribution of the $S_0 \rightarrow S_2$ transition for **1Az** is the HOMO → LUMO+1 transition, and that for **2Az** and **6Az** is the HOMO-1 → LUMO transition. This is because LUMO and LUMO+1 are near degenerate for **1Az** and HOMO and HOMO-1 are near degenerate for **2Az** and **6Az** (Figure 6). Moreover, the orbital pattern (Figure 6) shows that the electron distribution is localized in the three pairs only on the azulenyl moieties. Thus, both $S_0 \rightarrow S_1$ and $S_0 \rightarrow S_2$ transitions correspond to local excitations of the terminal azulenyl groups and have a similar character to the lowest-energy OPA transition of the unsubstituted azulene. This explains why the observed lowest-energy absorption bands (band I) of the azulenyl compounds are similar to the lowest-energy transition for unsubstituted azulene.

Contrary to these local excitations, transitions HOMO → LUMO+1 for **1Az** and HOMO-2 → LUMO for **2Az** and **6Az** are delocalized over the entire molecule (Figure 6). The excited states, for which these transitions play a dominant role, are S₃

for **1Az** and **2Az** and S₅ for **6Az**. These transitions have oscillator strengths larger than unity and the direction of the transition dipoles is parallel to the long molecular axis (Tables 3–5). Therefore, these transitions correspond to band II, which exhibits strong OPA and is a manifestation of the high degree of conjugation between the azulenyl moieties and the central $-\pi-A-\pi-$ moiety. The excitation energies and the relative magnitude of the oscillator strength (**1Az** > **2Az** > **6Az**) agree well with the experimental results for band II. This leads to the conclusion that the excited states corresponding to band II be assigned to S₃ for **1Az** and **2Az**, and S₅ for **6Az** (Figure 5).

Correspondence between the two experimentally observed OPA bands (bands I and II) and some calculated excited states has been established. Next, the excited states related to the TPA transition are considered. For this examination, it is worthy to recall the molecular symmetry and the selection rules that distinguish one- and two-photon transitions.⁶² For a centrosymmetric molecule, a TPA-allowed transition is forbidden for a one-photon process, and *vice versa* (*i.e.*, states populated by TPA will not be populated by OPA, and *vice versa*). For example, in the case of a C_{2h} molecule, the TPA-allowed $\pi-\pi^*$ excited states belong to A_g symmetry.⁴¹ In the present case, the azulenyl compounds are not rigidly centrosymmetric. However,

TABLE 5: One-Photon Absorption Properties of 6Az Calculated Using the TDDFT Method

<i>n</i>	excitation energy $\Delta E[S_n-S_0]$ (eV)	symmetry	orbital picture ^a	transition dipole moment (au)	oscillator strength
1	1.90	B	a(H) \rightarrow b(L) (0.91)	0.2071 (x)	0.0056
2	1.91	A	b(H-1) \rightarrow a(L+1) (-0.30)	-0.2796 (y)	0.0049
3	2.63	A	b(H-1) \rightarrow b(L) (0.91)	-0.3244 (z)	0.0022
4	2.63	B	a(H) \rightarrow a(L+1) (-0.30)	0.1869 (z)	0.0010
5	2.78	B	a(H) \rightarrow a(L+1) (0.92)	-0.1058 (x)	0.0017
6	2.78	A	b(H-1) \rightarrow b(L) (0.35)	-0.0675 (y)	1.1080
7	3.06	A	b(H-1) \rightarrow a(L+1) (0.92)	4.0346 (y)	0.0017
8	3.41	A	a(H) \rightarrow b(L) (0.34)	-0.1595 (z)	0.0163
			a(H-2) \rightarrow b(L) (0.92)	0.4663 (z)	0.0033
			b(H-4) \rightarrow b(L) (0.88)		
			b(H-3) \rightarrow b(L) (-0.37)		
			b(H-3) \rightarrow b(L) (0.81)		
			b(H-4) \rightarrow b(L) (0.38)		
			a(H-2) \rightarrow a(L+1) (-0.30)		
			a(H-2) \rightarrow a(L+1) (0.81)		
			b(H-1) \rightarrow b(L+2) (0.37)		
			a(H) \rightarrow a(L+3) (0.35)		

^a Values in parentheses are the coefficients of each electronic configuration contributing to the excited state. Configuration coefficients >0.3 are listed. Data for $n = 1-4$ and 8 show the transitions corresponding to local excitations.

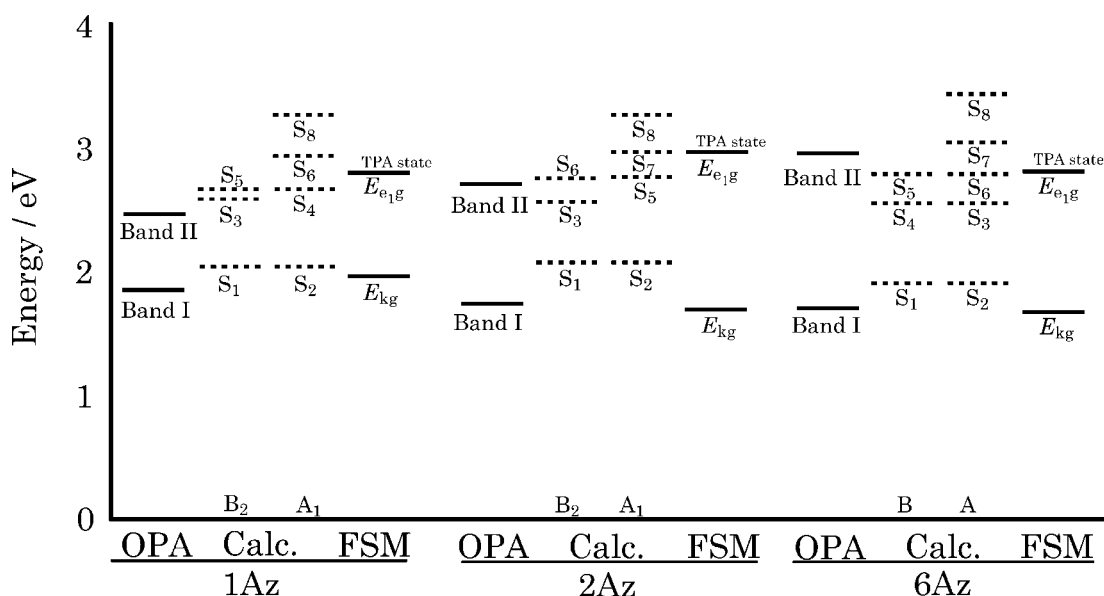


Figure 5. Energy diagrams of the examined compounds as estimated from one-photon absorption (OPA) measurements and TPA measurements with best-fits based on the four-state model (FSM), together with results calculated using the TDDFT method (Calc.). The ground states of the compounds are represented by 0.

the excited states are likely to be divided into mainly TPA-allowed and mainly OPA-allowed excited states. The mainly TPA-allowed excited states are expected to be A_1 (for the C_{2v} point group) or A (for the C_2 point group). In addition, the transitions related to the molecular orbital localized on azulenyl moieties are likely to be excluded as candidates for the major TPA-allowed excited states. This is because such transitions give much smaller TPA activity than the transition for the entire delocalized molecule, as the unsubstituted azulene gives no measurable signal. Thus, the first detectable TPA-allowed excited states of **1Az** and **2Az** can be assigned to S_6 and S_7 , respectively. In fact, the excitation energies of these states agree well with E_{e1g} obtained from the four-state model analysis (Figure 5). For **6Az**, there are two candidates, S_6 and S_7 , as the major TPA-allowed excited state. Both states consist of two transitions, $b(H-3) \rightarrow b(L)$ and $b(H-4) \rightarrow b(L)$. As seen in the orbital maps in Figure 6, $b(H-4)$ has a σ -orbital character, and the two transitions are considered to be mixed to form the

two states due to the deviation from the planar structure of the molecule. Among the two states, S_6 has the major component of the transition, $b(H-4) \rightarrow b(L)$, and has more character of the $\sigma-\pi^*$ transition such as S_7 of **1Az** or S_4 of **2Az**. It is plausible that S_6 does not have large absorption intensities for both OPA and TPA. Therefore, it is valid to consider that the first detectable TPA-allowed excited state of **6Az** should be S_7 , which has more character of the $\pi-\pi^*$ transition.

Effect of the Substitution Position of the Azulenyl Group.

As already described in the Introduction, it has been reported that when a position in the electron-rich five-membered ring is introduced into a π -conjugated system, the azulenyl moiety acts as a potential donor. On the one hand, when a position in an electron-deficient seven-membered ring is introduced into a π -conjugated system, the azulenyl moiety acts as a potential electron acceptor.⁵² On the basis of these concepts, the electronic features of **2Az** should be similar to those of **1Az**. However, OPA measurements and TDDFT calculations suggest that the


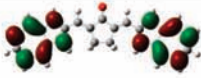
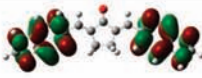

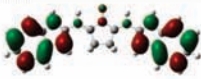
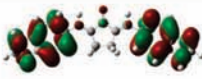

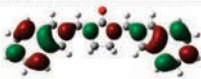
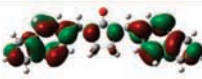
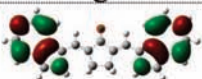



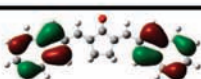
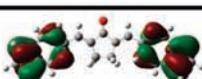

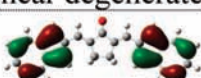
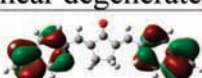









	1Az	2Az	6Az
LUMO+3	 a_2	 a_2	 a
LUMO+2	 b_1	 b_1	 b
LUMO+1	 a_2 (near degenerate)	 a_2	 a
LUMO	 b_1 (near degenerate)	 b_1	 b
HOMO	 a_2	 a_2 (near degenerate)	 a (near degenerate)
HOMO-1	 b_1	 b_1 (near degenerate)	 b (near degenerate)
HOMO-2	 b_2	 a_2	 a
HOMO-3	 a_2	 b_1	 b
HOMO-4	 b_1	 b_2	 b

Figure 6. Fine molecular orbital surfaces associated with the lower electronic transitions of the azulenyl compounds.

electronic properties of the azulene-2-yl group are different from that of the azulene-1-yl group, but rather similar to that of the azulene-6-yl group. For example, the MOs localized on the azulenyl moieties for **1Az** are LUMO and LUMO+1, and that for **2Az** and **6Az** are HOMO and HOMO-1. In addition, the 0-0 transition of band I for **1Az** is blue-shifted compared with

that for unsubstituted azulene, and those for **2Az** and **6Az** are red-shifted. The same trend was reported in a previous paper; that the 0-0 transitions in band I are red-shifted when azulene is substituted by a simple acceptor group at an even numbered position (2, 4, 6, or 8) and that they are blue-shifted when substituted at an odd numbered position (1, 3, 5, or 7).⁵⁸ This

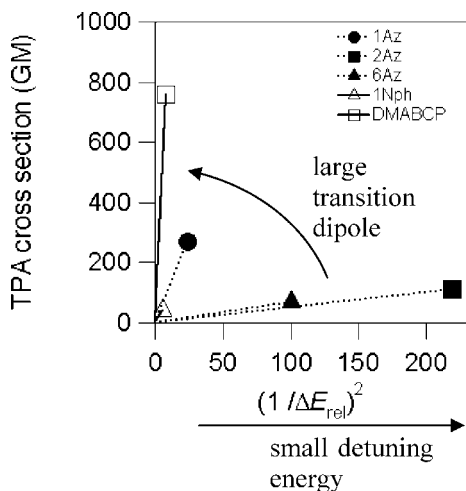


Figure 7. Relationship between the observed $\sigma_{\text{peak}}^{(2)}$ and the inverse square of the detuning energies (ΔE). In this plot, the slopes are proportional to $|\mu_{e_1,k}|^2|\mu_{k,g}|^2$. The slopes of **1Az**, **2Az**, **6Az**, **1Nph**, and **DMABCP** were estimated to be 12, 0.5, 0.7, 7 and 100, respectively.

suggests that the donor ability of the azulene-2-yl group is not so significant and is expected to be less than that of the azulene-1-yl group, but rather similar to that of the azulene-6-yl group. Therefore, it follows that the azulene-2-yl group acts as an acceptor rather than a donor in the azulene- π -A- π -azulene backbone.

As shown in Table 1, the oscillator strengths for band II were increased in the order **6Az** < **2Az** < **1Az**. Therefore, the transition dipole moments of azulenyl compounds $|\mu_{k,g}|$ should be increased in the order **6Az** < **2Az** < **1Az**. In the D- π -A- π -D backbone, the transition dipole moments were also increased with the increase of the donor strength of both terminal substituents. With respect to these observations, among the azulenyl groups, azulene-1-yl is quite likely to be an efficient electron donor group and azulene-6-yl is likely to be an acceptor group for a nonlinear optical compound.

To obtain greater insight regarding the difference in the TPA activity among these compounds, the observed $\sigma_{\text{peak}}^{(2)}$ values were plotted against the inverse square of the relative detuning energy $\Delta E_{\text{rel}} = (E_{k,g} - 1/2E_{e_1,g})/E_{e_1,g} = \Delta E/E_{e_1,g}$ (Figure 7). The theoretical expression for the $\sigma_{\text{peak}}^{(2)}$ of the lowest-energy TPA peak ($g \rightarrow e_1$) can be readily obtained from eq 1 by setting $E_{e_1,g} = 2E_p$ and by ignoring the second lowest TPA transition ($g \rightarrow e_2$) as follows^{21,41}

$$\sigma_{\text{peak}}^{(2)} \propto \frac{|\mu_{k,g}|^2|\mu_{e_1,k}|^2}{\Delta E_{\text{rel}}^2 \Gamma_{e_1,g}} \quad (2)$$

Equation 2 shows that the slopes of the plots in Figure 7 are proportional to the transition dipole product $|\mu_{k,g}|^2|\mu_{e_1,k}|^2$. Figure 7 illustrates that **1Az** has a larger detuning energy, which decreases $\sigma_{\text{peak}}^{(2)}$, compared to the other azulenyl compounds; however, the much larger transition dipole product overcomes the effect, resulting in a large $\sigma_{\text{peak}}^{(2)}$. The slopes increase in the order of **2Az** < **6Az** \ll **1Az**. By comparing the order of $|\mu_{k,g}|$ and assuming that $\Gamma_{e_1,k}$ is the same for all compounds, we find the transition dipole between the excited states $|\mu_{e_1,k}|$ of **1Az** is much larger than that of the other azulenyl compounds. This is considered to originate from the electron donating character of the azulene-1-yl group. These results demonstrate that not a simple azulenyl substitution at an arbitrary position but rather substitution at a specific position into a π -electron system is an

important factor for molecular design of an attractive TPA compound involving azulene.

Comparison with the Nonazulenyl Compounds. As shown in Table 2, the $\sigma_{\text{peak}}^{(2)}$ of all the azulenyl compounds were found to be larger than that of the conventional aromatic structural isomer **1Nph**; in particular, the $\sigma_{\text{peak}}^{(2)}$ of **1Az** was found to be 7 times larger. On the other hand, **DMABCP** exhibited the largest $\sigma_{\text{peak}}^{(2)}$ of all compounds the examined.

Figure 7 indicates that the slopes of the compounds treated in this study can be classified into three groups: (1) **DMABCP** with large slope and detuning energy, (2) **1Az** and **1Nph** with moderate slope and large detuning energy, and (3) **2Az** and **6Az** with small slope and detuning energy. In the case of **DMABCP**, the large transition dipole product gives a large $\sigma_{\text{peak}}^{(2)}$ in spite of the large detuning energy. On the other hand, **2Az** and **6Az** exhibit larger $\sigma_{\text{peak}}^{(2)}$'s than the benzenoid isomer **1Nph**, because of their small detuning energies. The slopes of **1Az** and **1Nph** were almost in the same order of magnitude. However, that of **1Az** was slightly larger than that of **1Nph**. In addition, the detuning energy of **1Az** was smaller than that of **1Nph**. These results show that the azulenyl compounds have larger $\sigma_{\text{peak}}^{(2)}$'s than the benzenoid isomer due to the small detuning energy. Therefore, it should be concluded that the introduction of an azulenyl group into a π -electron system is an effective strategy to obtain a compound with small ΔE , and thus large $\sigma_{\text{peak}}^{(2)}$.

Generally, the transition dipole moments of molecules based on the scheme D- π -A- π -D should be increased with increasing donor and/or acceptor strength.¹⁹ The slope of **1Az** was slightly larger than that of **1Nph** but is considerably smaller than that of **DMABCP**. These results suggest that the unsubstituted azulene-1-yl moiety acts as a weak donor in the D- π -A- π -D backbone. To obtain a superior TPA compound by utilizing the small detuning energy of azulenyl compounds, further structural modifications are required on the **1Az** backbone for enhancement of the donor ability and/or the transition dipole moment. For example, introduction of a strong donor, such as a dimethylamino moiety, at an effective position of the azulenyl moiety and/or the further extension of the π -electron system in the backbone should enhance $|\mu_{e_1,k}|^2|\mu_{k,g}|^2$.

4. Conclusions

We have investigated the TPA characteristics of newly synthesized conjugated ketone derivatives with three different azulenyl groups in a π -conjugated system. The OPA spectra of these azulenyl compounds were found to exhibit a weak absorption band in the wavelength region of 500–800 nm (band I), and an intense absorption band in the wavelength region of 300–520 nm (band II). TDDFT calculations indicated that the MO related to the former transition is localized at the azulenyl moieties, and the MO related to the latter transition is a well conjugated π -electron system over the entire molecule. It was found that the TPA cross sections of all the azulenyl compounds were larger than that of the benzenoid structural isomer **1Nph**. In particular, that of **1Az** was 7 times larger than that of **1Nph** at the lowest-energy TPA peak. It was determined that the reason for this can be primarily ascribed to the small ΔE of the azulenyl compounds. The present study demonstrates that azulenyl compounds possessing small ΔE are potentially promising TPA compounds. For further enhancement, modification of the molecular design is required to increase the transition dipole while maintaining a small ΔE .

Acknowledgment. S.H. was financially supported by JSPS Research Fellowships for Young Scientists. We thank the Media

and Information Technology Center of Yamaguchi University for the use of the PC cluster systems.

References and Notes

- (1) Maruo, S.; Nakamura, O.; Kawata, S. *Opt. Lett.* **1997**, *22*, 132.
- (2) Cumpston, B. H.; Ananthaval, S. P.; Barlow, S.; Dyer, D. L.; Ehrlich, J. E.; Erskine, L. L.; Heikal, A. A.; Kuebler, S. M.; Lee, I.-Y. S.; McCord-Maughon, D.; Qin, J.; Röckel, H.; Rumi, M.; Wu, X.-L.; Marder, S. R.; Perry, J. W. *Nature* **1999**, *398*, 51.
- (3) Guo, F.; Guo, R.; Jiang, Z.; Zhang, Q.; Huang, W.; Guo, B. *Phys. Stat. Sol. (a)* **2005**, *13*, 2515.
- (4) Perry, J. W.; Mansour, K.; Lee, I.-Y. S.; Wu, X.-L.; Bedworth, P. V.; Chen, C.-T.; Ng, D.; Marder, S. R.; Miles, P.; Wada, T.; Tani, M.; Sasabe, H. *Science* **1996**, *273*, 1533.
- (5) Spangler, C. W. *J. Mater. Chem.* **1999**, *9*, 2013.
- (6) Lei, H.; Wang, H. Z.; Wei, Z. C.; Tang, X. J.; Wu, L. Z.; Tung, C. H.; Zhou, G. Y. *Chem. Phys. Lett.* **2001**, *333*, 387.
- (7) Yang, Z.; Wu, Z.; Ma, J.; Xia, A.; Li, Q.; Liu, C.; Gong, Q. *Appl. Phys. Lett.* **2005**, *86*, 061903.
- (8) Li, S. L.; Wu, J. Y.; Tian, Y. P.; Tang, Y. W.; Jiang, M. H.; Fun, H. K.; Chantapromma, S. *Opt. Mater.* **2006**, *28*, 897.
- (9) Parthenopoulos, D. A.; Rentzepis, P. M. *Science* **1989**, *245*, 843.
- (10) Strickler, J. H.; Webb, W. W. *Adv. Mater.* **1993**, *5*, 479.
- (11) Kawata, S.; Kawata, Y. *Chem. Rev.* **2000**, *100*, 1777.
- (12) Shiono, T.; Itoh, T.; Nishino, S. *Jpn. J. Appl. Phys.* **2005**, *44*, 3559.
- (13) Ishow, E.; Brosseau, A.; Clavier, G.; Nakatani, K.; Pansu, R. B.; Vachon, J.-J.; Tauc, P.; Chauvat, D.; Mendonça, C. R.; Piovesan, E. *J. Am. Chem. Soc.* **2007**, *129*, 8970.
- (14) Corredor, C. C.; Huang, Z.-L.; Belfield, K. D.; Morales, A. R.; Bondar, M. V. *Chem. Mater.* **2007**, *19*, 5165.
- (15) Denk, W.; Strickler, J. H.; Webb, W. W. *Science* **1990**, *248*, 73.
- (16) Abe, Y.; Toda, Y.; Hoshino, K.; Arakawa, Y. *Jpn. J. Appl. Phys.* **2005**, *44*, L535.
- (17) Bhawalker, J. D.; Kumar, N. D.; Zhao, C. F.; Prasad, P. N. *J. Clin. Laser Med. Surg.* **1997**, *15*, 201.
- (18) Ogawa, K.; Hasegawa, H.; Inada, Y.; Kobuke, Y.; Inouye, H.; Kanemitsu, Y.; Kohno, E.; Hirano, T.; Ogura, S.; Okura, I. *J. Med. Chem.* **2006**, *49*, 2276.
- (19) Albota, M.; Beljonne, D.; Brédas, J. L.; Ehrlich, J. E.; Fu, J. Y.; Heikal, A. A.; Hess, S. E.; Kogej, T.; Levin, M. D.; Marder, S. R.; Maughon, D. M.; Perry, J. W.; Röckel, H.; Rumi, M.; Subramaniam, G.; Webb, W. W.; Wu, X. L.; Xu, C. *Science* **1998**, *281*, 1653.
- (20) Reinhardt, B. A.; Brott, L. L.; Clarkson, S. J.; Dillard, A. G.; Bhatt, J. C.; Kannan, R.; Yuan, L.; He, G. S.; Prasad, P. N. *Chem. Mater.* **1998**, *10*, 1863.
- (21) Rumi, M.; Ehrlich, J. E.; Heikal, A. A.; Perry, J. W.; Barlow, S.; Hu, Z.; McCord-Maughon, D.; Parker, T. C.; Röckel, H.; Thayumanavan, S.; Marder, S. R.; Beljonne, D.; Brédas, J. L. *J. Am. Chem. Soc.* **2000**, *122*, 9500.
- (22) Belfield, K. D.; Schafer, K. J.; Mourad, W.; Reinhardt, B. A. *J. Org. Chem.* **2000**, *65*, 4475.
- (23) Kim, K.; Lee, K. S.; Woo, H. Y.; Kim, K. S.; He, G. S.; Swiatkiewicz, J.; Prasad, P. N. *Chem. Mater.* **2000**, *12*, 284.
- (24) Mongin, O.; Brunel, J.; Porres, L.; Blanchard-Desce, M. *Tetrahedron Lett.* **2003**, *44*, 2813.
- (25) Ogawa, K.; Ohashi, A.; Kobuke, Y.; Kamada, K.; Ohta, K. *J. Am. Chem. Soc.* **2003**, *125*, 13356.
- (26) Kawamata, J.; Akiba, M.; Inagaki, Y. *Jpn. J. Appl. Phys.* **2003**, *42*, L17.
- (27) Abboto, A.; Beverina, L.; Bradamante, S.; Facchetti, A.; Pagani, G. A.; Bozio, R.; Ferrante, C.; Pedron, D.; Signorini, R. *Synth. Mat.* **2003**, *136*, 795.
- (28) Kamada, K.; Ohta, K.; Iwase, Y.; Kondo, K. *Chem. Phys. Lett.* **2003**, *372*, 386.
- (29) De Boni, L.; Constantino, C. J. L.; Misoguti, L.; Aroca, R. F.; Zilio, S. C.; Mendonça, C. R. *Chem. Phys. Lett.* **2003**, *371*, 744.
- (30) Martineau, C.; Lemerrier, G.; Andraud, C.; Wang, I.; Bourriau, M.; Baldeck, P. L. *Synth. Mat.* **2003**, *138*, 353.
- (31) Zojer, E.; Beljonne, D.; Pacher, P.; Brédas, J. L. *Chem. Eur. J.* **2004**, *10*, 2668.
- (32) Karotki, A.; Drobizhev, M.; Dzenis, Y.; Taylor, P. N.; Anderson, H. L.; Rebane, A. *Phys. Chem. Chem. Phys.* **2004**, *6*, 7.
- (33) Zojer, E.; Beljonne, D.; Pacher, P.; Brédas, J. *Chem. Eur. J.* **2004**, *10*, 2668.
- (34) Belfield, K. D.; Bondar, M. V.; Przhonska, O. V.; Schafer, K. J. *J. Photochemistry and Photobiology A* **2004**, *162*, 489.
- (35) Katan, C.; Terenziani, F.; Mongin, O.; Werts, M. H. V.; Porrés, L.; Pons, T.; Mertz, J.; Tretiak, S.; Blanchard-Desce, M. *J. Phys. Chem. A* **2005**, *109*, 3024.
- (36) Ogawa, K.; Ohashi, A.; Kobuke, Y.; Kamada, K.; Ohta, K. *J. Phys. Chem. B* **2005**, *109*, 22003.
- (37) Kim, D. Y.; Ahn, T. K.; Kwon, J. H.; Kim, D.; Ikeue, T.; Aratani, N.; Osuka, A.; Shigeiwa, M.; Maeda, S. *J. Phys. Chem. A* **2005**, *109*, 2996.
- (38) Badaeva, E. A.; Timofeeva, T. V.; Masunov, A.; Tretiak, S. *J. Phys. Chem. A* **2005**, *109*, 7276.
- (39) Cohanoschi, I.; Belfield, K. D.; Hernández, F. E. *Chem. Phys. Lett.* **2005**, *406*, 462.
- (40) Akiba, M.; Morinaga, N.; Takizawa, H.; Ogiyama, M.; Ichijima, S.; Tani, T.; Harada, A.; Inagaki, Y. *Nonlinear Opt., Quantum Opt.* **2005**, *34*, 179.
- (41) Ohta, K.; Kamada, K. *J. Chem. Phys.* **2006**, *124*, 124303.
- (42) Morales, A. R.; Belfield, K. D.; Hales, J. M.; Van Stryland, E. W.; Hagan, D. J. *Chem. Mater.* **2006**, *18*, 4972.
- (43) Drobizhev, M.; Stepanko, Y.; Rebane, A.; Wilson, C. J.; Screen, T. E. O.; Anderson, H. L. *J. Am. Chem. Soc.* **2006**, *128*, 12432.
- (44) Ahn, T. K.; Kim, K. S.; Kim, D. Y.; Noh, S. B.; Aratani, N.; Ikeda, C.; Osuka, A.; Kim, D. *J. Am. Chem. Soc.* **2006**, *128*, 1700.
- (45) Terenziani, F.; Painelli, A.; Katan, C.; Charlot, M.; Blanchard-Desce, M. *J. Am. Chem. Soc.* **2006**, *128*, 15742.
- (46) Fortrie, R.; Anémian, R.; Stephan, O.; Mulatier, J.-C.; Baldeck, P. L.; Andraud, C.; Chermette, H. *J. Phys. Chem. C* **2007**, *111*, 2270.
- (47) Mongin, O.; Porrés, L.; Charlot, M.; Katan, C.; Blanchard-Desce, M. *Chem. Eur. J.* **2007**, *13*, 1481.
- (48) Tobler, H. J.; Bauder, A.; Günthare, H. H. *J. Mol. Spectrosc.* **1965**, *18*, 239.
- (49) Mann, D. E.; Platt, J. R.; Klevens, H. B. *J. Chem. Phys.* **1949**, *17*, 481.
- (50) Kurotobi, K.; Suk Kim, K.; Bum Noh, S.; Kim, D.; Osuka, A. *Angew. Chem., Int. Ed.* **2006**, *45*, 3944.
- (51) Kawamata, J.; Inoue, K.; Inabe, T. *Bull. Chem. Soc. Jpn.* **1998**, *71*, 2777.
- (52) Cristian, L.; Sasaki, I.; Lacroix, P. G.; Donnadiou, B.; Asselberghs, I.; Clays, K.; Razus, A. C. *Chem. Mater.* **2004**, *16*, 3543.
- (53) Asato, E.; Liu, R. S. H.; Rao, V. P.; Cai, Y. M. *Tetrahedron Lett.* **1996**, *37*, 419.
- (54) Iftimie, G.; Lacroix, P. G.; Nakatani, K.; Razus, A. C. *Tetrahedron Lett.* **1998**, *39*, 6853.
- (55) Sheik-Bahae, M.; Said, A. A.; Wei, T. H.; Hagan, D. J.; Van Stryland, E. W. *IEEE J. Quantum Electron.* **1990**, *26*, 760.
- (56) Kamada, K.; Matsunaga, K.; Yoshino, A.; Ohta, K. *J. Opt. Soc. Am. B* **2003**, *20*, 529.
- (57) Frisch, M. J.; Trucks, G. W.; Schlegel, H. B.; Scuseria, G. E.; Robb, M. A.; Cheeseman, J. R.; Montgomery, Jr., J. A.; Vreven, T.; Kudin, K. N.; Burant, J. C.; Millam, J. M.; Iyengar, S. S.; Tomasi, J.; Barone, V.; Mennucci, B.; Cossi, M.; Scalmani, G.; Rega, N.; Petersson, G. A.; Nakatsuji, H.; Hada, M.; Ehara, M.; Toyota, K.; Fukuda, R.; Hasegawa, J.; Ishida, M.; Nakajima, T.; Honda, Y.; Kitao, O.; Nakai, H.; Klene, M.; Li, X.; Knox, J. E.; Hratchian, H. P.; Cross, J. B.; Bakken, V.; Adamo, C.; Jaramillo, J.; Gomperts, R.; Stratmann, R. E.; Yazyev, O.; Austin, A. J.; Cammi, R.; Pomelli, C.; Ochterski, J. W.; Ayala, P. Y.; Morokuma, K.; Voth, G. A.; Salvador, P.; Dannenberg, J. J.; Zakrzewski, V. G.; Dapprich, S.; Daniels, A. D.; Strain, M. C.; Farkas, O.; Malick, D. K.; Rabuck, A. D.; Raghavachari, K.; Foresman, J. B.; Ortiz, J. V.; Cui, Q.; Baboul, A. G.; Clifford, S.; Cioslowski, J.; Stefanov, B. B.; Liu, G.; Liashenko, A.; Piskorz, P.; Komaromi, I.; Martin, R. L.; Fox, D. J.; Keith, T.; Al-Laham, M. A.; Peng, C. Y.; Nanayakkara, A.; Challacombe, M.; Gill, P. M. W.; Johnson, B.; Chen, W.; Wong, M. W.; Gonzalez, C.; Pople, J. A. *Gaussian 03*, Revision D.02; Gaussian, Inc.: Wallingford, CT, 2004.
- (58) Shevyakov, S. V.; Li, H.; Muthyala, R.; Asato, A. E.; Croney, J. C.; Jameson, D. M.; Liu, R. S. H. *J. Phys. Chem. A* **2003**, *107*, 3295.
- (59) Kawamata, J.; Inoue, K.; Kasatani, H.; Terauchi, H. *Jpn. J. Appl. Phys.* **1992**, *31*, 254.
- (60) Kawamata, J.; Inoue, K. *Mol. Cryst. Liq. Cryst.* **1996**, *278*, 117.
- (61) Woo, H. Y.; Liu, B.; Kohler, B.; Korystov, D.; Mikhailovsky, A.; Bazan, G. C. *J. Am. Chem. Soc.* **2005**, *127*, 14721.
- (62) Arnbjerg, J.; Paterson, M. J.; Nielsen, C. B.; Jørgensen, M.; Christiansen, O.; Ogilby, P. R. *J. Phys. Chem. A* **2007**, *111*, 5756.